


RESEARCH ARTICLE

Wide-temperature range thermoregulating e-skin design through a hybrid structure of flexible thermoelectric devices and phase change materials heat sink

Pengxiang Zhang^{1,2}  | Biao Deng¹ | Kang Zhu¹ | Qing Zhou¹ |
Shuangmeng Zhang¹ | Wenting Sun^{1,3} | Zijian Zheng^{2,4,5} | Weishu Liu^{1,3}

¹Department of Materials Science and Engineering, Southern University and Science and Technology, Shenzhen, China

²Institute of Textiles and Clothing, The Hong Kong Polytechnic University, Hong Kong SAR, China

³Shenzhen Engineering Research Center for Novel Electronic Information Materials and Devices, Southern University of Science and Technology, Shenzhen, China

⁴Research Institute for Intelligent Wearable Systems, The Hong Kong Polytechnic University, Hong Kong SAR, China

⁵Research Institute for Smart Energy, The Hong Kong Polytechnic University, Hong Kong SAR, China

Correspondence

Weishu Liu, Department of Materials Science and Engineering, Southern University and Science and Technology, Shenzhen 518055, China.
Email: liuws@sustech.edu.cn

Funding information

Guangdong Province Introduction of Innovative R&D Team, Grant/Award Number: 2016ZT06G587; Hong Kong Polytechnic University, Grant/Award Number: ZVQM; RGC Senior Research Fellow Scheme, Grant/Award Number: SRFS2122-5S04; Shenzhen Science and Technology Program, Grant/Award Numbers: KYDPT20181011104007, GXWD20201230110313001

Abstract

The realization of the thermoregulating function of electronic skin (e-skin) by simulating the human temperature perception system can greatly improve the intelligence of the e-skin. Here, we report a thermoregulating e-skin that fits on the surface of a prosthetic limb based on a hybrid structure consisting of a flexible thermoelectric device and a phase-change heat sink. The hybrid e-skin possesses outstanding temperature adaptability similar to that of the human body; it can maintain the surface temperature at 35°C in environmental temperatures ranging from 10 to 45°C. The power expenditure of the e-skin is essentially the same as the energy required by the human body to regulate temperature and is only 14.22 mW cm⁻² in the thermoneutral zone. Thermoregulation based on this e-skin can greatly improve the temperature distribution of the target surface, providing a promising solution for the biomimetic thermoregulation of robots and the next generation of intelligent prostheses.

KEYWORDS

e-skin, phase change material, thermoelectric device, thermoregulation

1 | INTRODUCTION

The skin, the largest organ of the human body, is stretchable and strong enough to protect the organs inside the body; at the same time, the skin is also

sensitive to the environment through various tactile sensory receptors.^{1–3} In recent years, electronic skins (e-skins) with protection, perception, and adjustment functions have been developed, which show promising applications in wearable devices, human-computer

This is an open access article under the terms of the [Creative Commons Attribution](https://creativecommons.org/licenses/by/4.0/) License, which permits use, distribution and reproduction in any medium, provided the original work is properly cited.

© 2022 The Authors. *EcoMat* published by The Hong Kong Polytechnic University and John Wiley & Sons Australia, Ltd.

interface, intelligent prostheses, medical diagnostics, and other areas.^{4–9}

The temperature sensing and thermoregulating function of e-skin is attracting increasing attention, particularly in the intellectualization of bionic robots and mechanical prostheses.^{10–12} Human beings perceive different degrees of heat and cold through four types of temperature sensory receptors.¹³ The human body has an integrated secretion system and heat production mechanism capable of maintaining body temperature within a thermostatic state, regardless of surrounding conditions.¹⁴ The classic e-skin, on the other hand, due to limitations of materials and structures, cannot maintain a constant temperature like the human body can in a temperature-varying environment. Similar to the heterothermal animal, the temperature of the classic e-skin is passively associated with the ambient temperature.¹⁵ The lack of temperature regulation of the e-skin cannot only endanger the user of e-skin but may also induce negative psychological outcomes. For example, if the human body comes into contact with the e-skin attached to the prosthesis surface, the temperature difference between the human skin and the e-skin will make the human body feel uncomfortable, which impedes the amputee's acceptance of the prosthesis. As a result, a thermoregulating design for the e-skin is critical as this could significantly increase the comfortability of assist prosthetic users, and rebuild up their self-confidence.

The purpose of thermoregulating design is to influence the temperature of an object by adjusting heat transfer, including enhanced heat dissipation and suppressed heat loss, to improve the object's thermal environment.^{16–18} For heat dissipation, materials of high thermal conductivity can swiftly dissipate the Joule heat generated by functional electronics.^{19–21} As an alternative way to prevent high temperatures, phase change materials (PCM) such as paraffin are used to regulate temperature near the phase change temperature point.^{22–24} Control of thermal radiation using infrared transparent or reflective textiles was reported for personal thermal management.^{25–28} However, these passive thermal management strategies using high thermal conductivity materials, PCM, and thermal management textiles, are only suitable for single-purpose heating or cooling, but not both. For thermoregulation, an active means is essential to control the temperature in a varying thermal environment. Active thermoregulation involves connecting an external power supply, converting electric energy to heat energy, and then changing the temperature of the object. Using the joule effect of conductors to change temperature is an efficient heating method.^{29–32} Thermoelectric techniques can create a temperature gradient on the device for heating and cooling based on the Peltier

effect.^{33–36} However, there is no report on how to accurately regulate the temperature of e-skin in a complicated thermal environment.

To address this challenge, we propose a wide-temperature range thermoregulating e-skin design based on a hybrid structure consisting of flexible thermoelectric devices and phase-change heat sinks. The e-skin is mounted to a prosthetic limb as the surface skin for thermoregulation. We systematically investigated the thermoregulating performance of the hybrid e-skin in both hot and cold environments. We discussed the power expenditure to maintain the e-skin at a comfortable temperature. The e-skin maintained the surface temperature at 35°C in temperatures ranging from 10 to 45°C. The hybrid e-skin provides a solution for biomimetic temperature regulation in robotics and the next generation of intelligent prostheses.

2 | RESULTS AND DISCUSSION

2.1 | Thermoregulating design of an e-skin through a hybrid structure

Figure 1 shows the concept of a wide-temperature range thermoregulating e-skin design. Humans are homeothermic, in contrast to heterothermal animals such as the bullfrog (Figure 1A).^{13–15} Humans maintain an almost constant body temperature through autonomic and behavioral responses that provide thermoregulation. As a result of thermoregulatory behavioral responses, humans will naturally seek a state of thermal comfort. Thermoregulation also affords us the ability to be highly sensitive to environmental changes and express our emotions. To mimic thermoregulation of the body, we used a hybrid structure consisting of a flexible thermoelectric device and a PCM heat sink (Figure 1B,C). We used an island-bridge structure to assemble the flexible thermoelectric device (detailed steps are provided in Section 4). The as-fabricated flexible thermoelectric device could bend and conform well to a prosthetic limb surface. To lengthen the cooling service life of the thermoelectric devices, a paraffin/organosilicone composite was used for the PCM heat sinks. The PCM can absorb a substantial amount of heat while maintaining a constant temperature as the temperature of the hot side approaches the phase change point of the PCM, extending the thermoelectric device's effective cooling duration. Figure S1A shows the simulation results for mechanical properties of flexible thermoelectric devices in both traditional and island-bridge configurations. When a negative z-axis force of 0.02 N was applied to the right side of the device, the maximum displacement of the conventional configuration was

about 74 μm . Under the same stress conditions, the maximum displacement of the island-bridge configuration was 0.89 mm, which is one order of magnitude larger than that of the traditional configuration, indicating that the overall flexibility of the island bridge configuration is significantly better than that of the traditional configuration. The as-fabricated e-skin is durable in cyclic bending, showing almost no change in resistance after 200 bending cycles (Figure S1B).

The human skin can regulate body temperature even in complicated temperature environments, in part because cells create a substantial quantity of heat through metabolism to keep the human body temperature near 37°C and sustain normal physiological processes of the human body. Figure 1D,E show the home-built wind channel for simulating a hot or cold environment with controllable wind speed and temperature. For the thermoregulating performance measurement, the as-fabricated

hybrid e-skin was set on a silicone-based prosthesis in the wind channel. The heating, cooling, and temperature adaptation effects of the e-skin in complex environments were systematically investigated as described in the next sections.

2.2 | Thermoregulation of hybrid e-skin in a cold environment

In a cold environment, cold receptors in the skin of humans perceive cold temperatures and convey signals to the brain, resulting in the sensation of cold (Figure 2A). The brain controls processes that decrease heat loss through the skin, such as vasoconstriction and contraction of the arrector pili muscles.¹⁴ In the as-fabricated hybrid e-skin, the temperature sensor, similar to a human body temperature receptor, monitors temperature

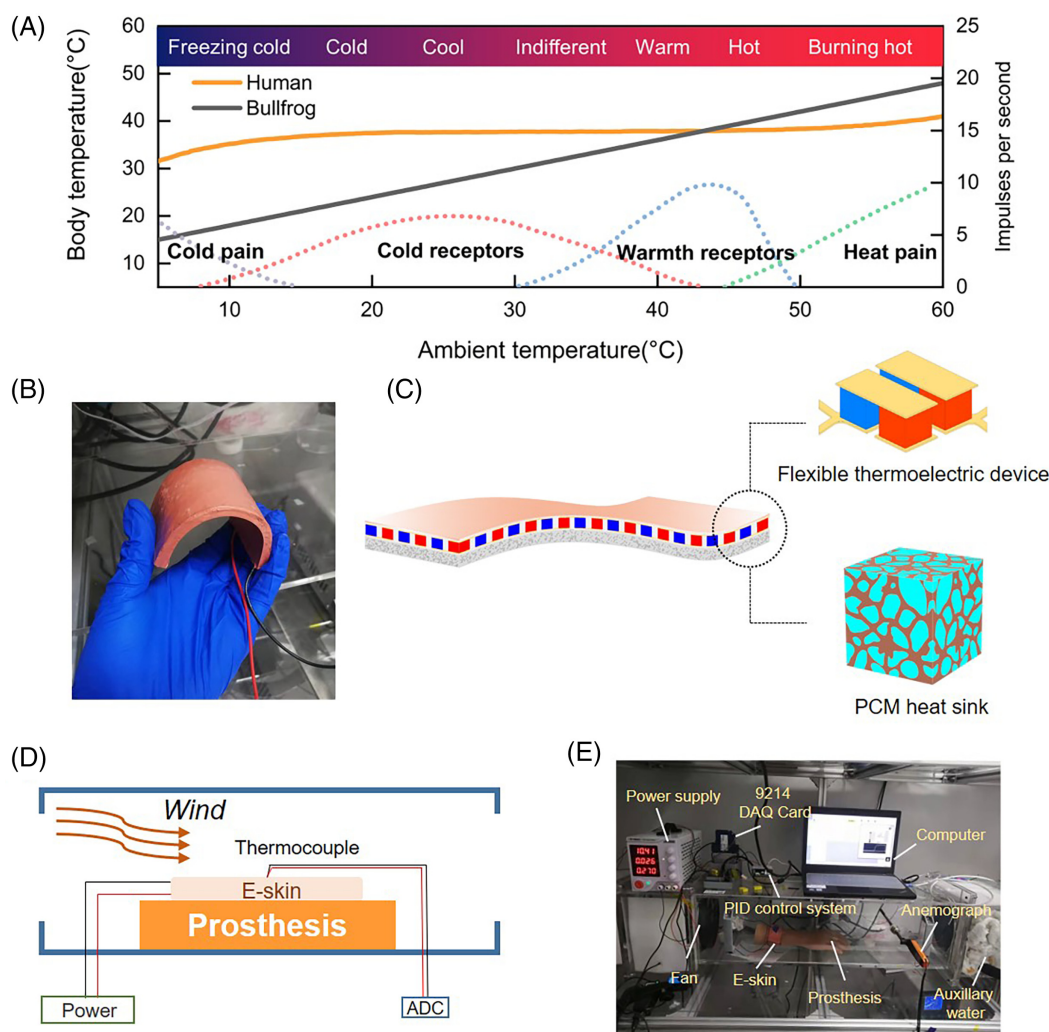


FIGURE 1 The design and testing equipment of the e-skin. (A) The body's sense of temperature and the need for temperature regulation^{13–15}; (B) photo of the thermoregulating e-skin; (C) basic structure of the thermoregulating e-skin; (D) test schematic diagram of the temperature control experiment; (E) photo of the experimental test equipment

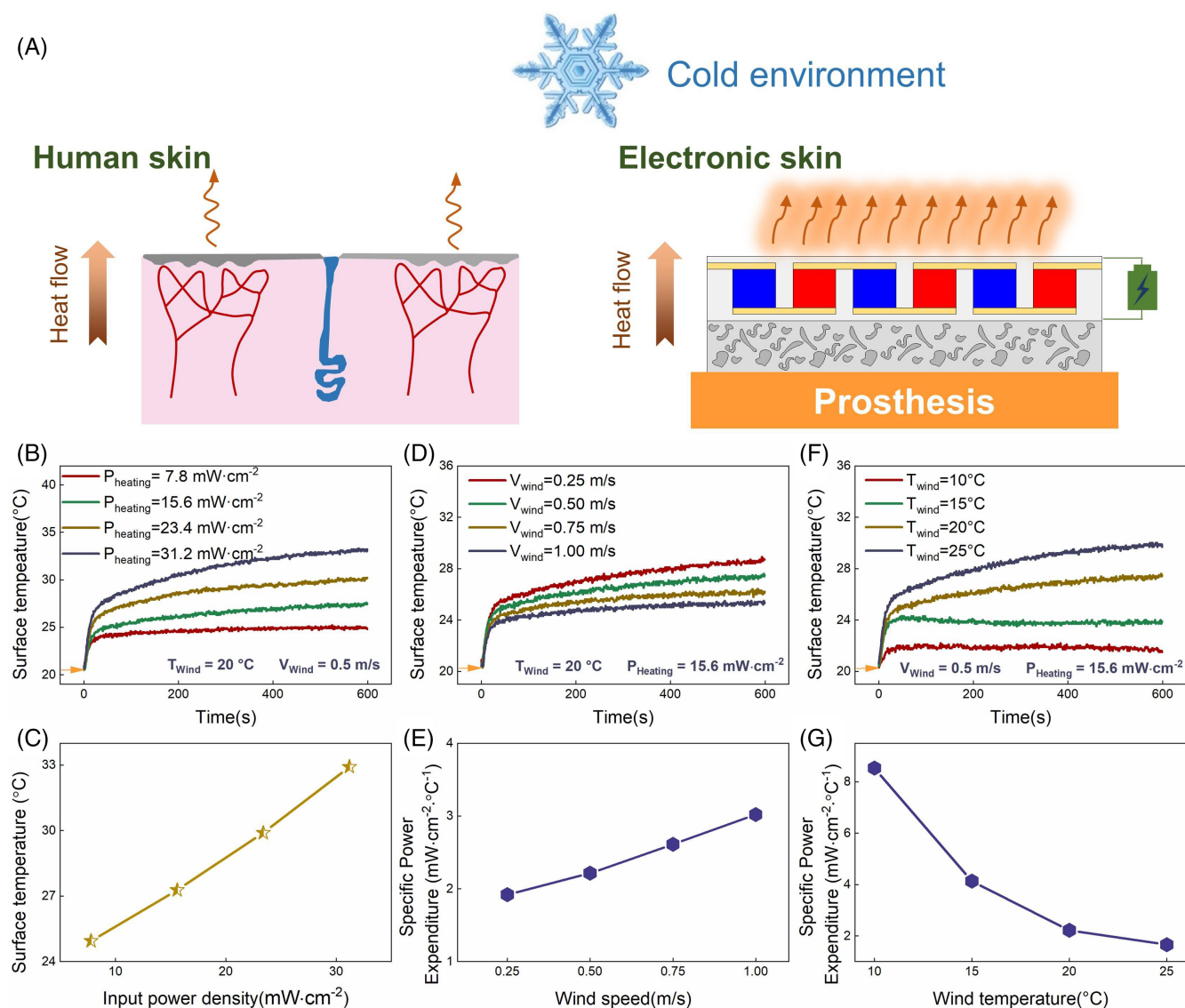


FIGURE 2 Thermoregulation of the e-skin in a cold environment. (A) Temperature regulation of human skin and e-skin in a low-temperature environment; (B) and (C) are the surface temperatures of the e-skin under different input power densities; (D) and (E) are the surface temperatures and the specific power expenditures of the e-skin under different wind speeds; (F) and (G) are the surface temperatures and the specific power expenditures of the e-skin under different wind temperatures

drops and sends the signal to the control system to turn on the power of the thermoelectric unit. The e-skin then undergoes a heating process.

Figure 2B,C present the effect of input power density on the surface temperature of the e-skin exposed to an ambient temperature of 20°C and a wind speed of 0.5 m s^{-1} . With an input power density of 7.8 mW cm^{-2} , the e-skin surface temperature first rises rapidly, then slowly until it reaches 24.8°C after 600 s. An increase in the input power density increases the e-skin heat production, which raises the e-skin surface temperature. Under an input power density of 31.2 mW cm^{-2} , the e-skin surface temperature was stable at 32.9°C . By changing the input power to affect heat production, the surface

temperature of the e-skin can be heated to the desired temperature.

Body thermoregulation involves a balance between heat production and heat dissipation.¹⁴ We imitated human body to explore the thermoregulating effect of e-skin under different heat dissipation conditions when the input power density is constant. We define specific power expenditure (the e-skin thermoregulating power density requirements to change the surface temperature per degree Celsius) to determine the thermoregulating effect of e-skin. Figure 2D,E illustrate the e-skin's surface temperature measured and the specific power expenditure under various wind speeds, respectively. The stable surface temperature of the e-skin was 28.7°C at low wind speed

(0.25 m s^{-1}), but only 25.3°C at high wind speed (1 m s^{-1}) under the same conditions ($P_{\text{heating}} = 15.6 \text{ mW cm}^{-2}$, $T_{\text{wind}} = 20^\circ\text{C}$). And at a wind speed of 1 m s^{-1} , the specific power expenditure of the e-skin was $3 \text{ mW cm}^{-2} ^\circ\text{C}^{-1}$, 1.5 times higher than a wind speed of 0.25 m s^{-1} . The increasing wind speed increases the convective heat transfer between the e-skin surface and the environment. Similar to the human body, at low temperatures, strong convection conditions can remove more heat from the surface of the e-skin, requiring greater specific power expenditure to maintain surface temperature.

The thermoregulating ability of the e-skin was also affected by changing the wind temperature (Figure 2F, G). At the same wind speed and the same input power density, the stable surface temperature of the e-skin was 21.5°C at a wind temperature of 10°C , which was about 8°C lower than that when the wind temperature was 25°C . Consistently, the specific power expenditure increased from 1.66 to $8.53 \text{ mW cm}^{-2} ^\circ\text{C}^{-1}$ as the wind temperature declined from 25 to 10°C . The low temperature environment creates a larger temperature gradient with the e-skin surface, which increases the heat dissipation of the e-skin surface and impairs the heating ability of the e-skin. Greater specific power expenditure is required to raise the surface temperature of the e-skin when it is exposed to low temperatures.

In general, the e-skin adapts well to cold temperatures by heating and is affected by both internal and external heat transfer. When the environment is mild, the e-skin, like the human body, can raise surface temperature at a low specific power expenditure. The heating effect is weakened and the specific power expenditure rises when heat production is limited and heat dissipation is intense. This scenario can be altered by adjusting the e-skin input power density.

2.3 | Thermoregulation of hybrid e-skin in a hot environment

In a hot environment, the skin senses temperature through warm receptors and relays the information to the brain, resulting in the sensation of being hot. As shown in Figure 3A, the brain directs the skin tissue to execute cooling operations such as vasodilation, relaxation of arrector pili muscles, and perspiration.¹⁴ In a similar manner, when the temperature sensor in the thermoregulating e-skin detects that the external environment is too hot, it sends a signal to the control system. The thermoelectric device's upper surface is now the cold side, absorbing heat from the lower surface and cooling the e-skin surface. During this process, the thermoelectric device's lower surface is producing substantial heat,

therefore reducing the device's cooling effect. Human skin can radiate heat into the environment, but because the e-skin cannot do so, it must store heat in a heat reservoir beneath it to maintain a cooling effect on the surface.

Figure 3B,C show the effect of the input power density on the e-skin surface temperature when the ambient temperature was 35°C and the wind speed was 0.5 m s^{-1} . The surface temperature of the e-skin dropped with time when the input power density was 7.8 mW cm^{-2} , reaching a final temperature of 32°C . The e-skin surface temperature gradually dropped when the input power density increased. The surface temperature reached 29°C when the power density was 31.2 mW cm^{-2} , but eventually, the heat generation of hot side exceeded the phase change material's storage capacity, and the cooling effect of the thermoelectric device deteriorated. The surface temperature of the e-skin gradually increased to a final temperature of 32°C . The cooling effect of e-skin is affected by the heat generated by the hot side of thermoelectric device, which can be enhanced by improving the thermal conductivity of prostheses or increasing the heat storage of PCM in future.

In a high temperature environment, the surface of the e-skin undergoes a cooling process and its temperature is lower than that of the environment. The heat in the environment will affect the surface temperature of the e-skin through convection. We also measured the effect of different environmental conditions on the cooling performance of the e-skin. Figure 3D,E show the surface temperature and the corresponding specific power expenditure of the e-skin at various wind speeds. When the wind temperature was 35°C and the input power density was 15.6 mW cm^{-2} , the surface temperature of the e-skin decreased rapidly from 35 to 30°C at a wind speed of 0.25 m s^{-1} , and then remained relatively constant. At this time, the specific power expenditure of the e-skin was $3.3 \text{ mW cm}^{-2} ^\circ\text{C}^{-1}$. However, when the wind speed increased to 1 m s^{-1} , the final temperature of the e-skin increased to 32°C , and the specific power expenditure rose to $5.2 \text{ mW cm}^{-2} ^\circ\text{C}^{-1}$. The increase in wind speed enhanced convection between the e-skin surface and the environment, so greater specific power was required to lower the surface temperature.

In addition, e-skin cooling was hampered by rising ambient temperatures (Figure 3F,G). At a wind temperature of 30°C , the surface temperature of the e-skin was reduced from an initial 35°C down to 30°C and then remain constant, and the specific power expenditure of the e-skin was $3.3 \text{ mW cm}^{-2} ^\circ\text{C}^{-1}$. However, at the same power density and wind speed, but with the wind temperature increased to 45°C , the final temperature of the

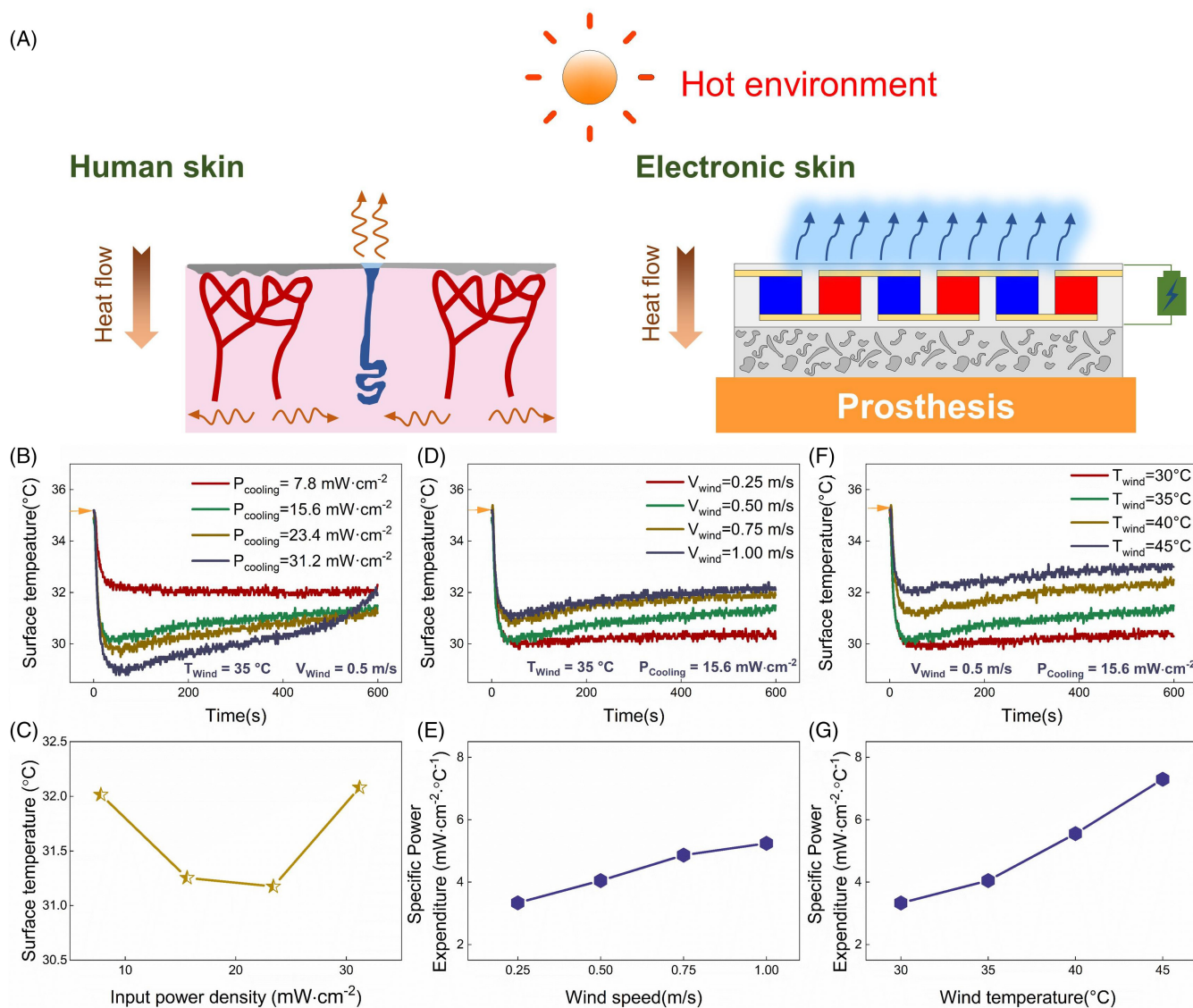


FIGURE 3 Thermoregulation of the e-skin in a hot environment. (A) Temperature regulation of human skin and e-skin in a high-temperature environment; (B) and (C) are the surface temperatures of the e-skin under different input power densities; (D) and (E) are the surface temperatures and the specific power expenditures of the e-skin under different wind speeds; (F) and (G) are the surface temperatures and the specific power expenditures of the e-skin under different wind temperatures

e-skin was 33°C, and the specific power expenditure of the e-skin was up to 7.3 mW cm⁻² °C⁻¹. Cooling the e-skin surface under high temperatures takes more energy when other factors remain constant.

The cooling function of the e-skin is affected by heat transmission. High temperature environments and fast wind speeds enhance heat transmission between the e-skin and the environment, limiting the cooling effect of the e-skin. The specific power expenditure is determined by the degree of heat transmission between the e-skin surface and the environment. The higher the heat transmission rate, the greater specific power expenditure is required.

2.4 | Temperature adaptation performance of hybrid e-skin

The as-fabricated e-skin has been shown to provide single-purpose thermoregulation in various cold and hot environments, with a corresponding specific power expenditure. To realize automatic control of the e-skin surface temperature, a proportional-integral-derivative (PID) control system was adopted to achieve feedback thermoregulation. Human skin temperature varies with the season and environment, and approximately 31.5–35.5°C is considered to be a comfortable skin temperature.^{37,38} Here, we chose 35°C as the target temperature

of the e-skin. However, humans have limited energy and seek an ideal environment based on their personal preferred temperature.³⁹ This behavior is driven by the goal to minimize the temperature gradient between the environment and the person to reduce the temperature difference between them. To maintain body temperature, this strategy enables people to use less metabolic energy. Similarly, when the hybrid e-skin is used on a prosthetic limb or robot, the amount of energy it can store to support thermoregulation is limited. Here, we define the temperature adaptation capacity as the maximum time the e-skin can maintain its surface temperature at 35°C when the power supply is limited, which is related to the power expenditure and effective time of the e-skin temperature regulation. At low temperatures, the effective time of the e-skin can be indefinite. However, as temperature decreases, the e-skin power expenditure required to regulate temperature increases, and the period during which the e-skin can regulate temperature is shorter when energy is limited. Therefore, the temperature adaptation capacity of the e-skin gradually decreases with a decrease of temperature when the ambient temperature is lower than the target temperature. In the high temperature environment, the temperature adaptation of e-skin is restricted by the heat storage of PCM, causing the effective period of the e-skin temperature adaptation to

decrease as the ambient temperature increases. As a result, the higher the ambient temperature, the weaker the temperature adaptation of the e-skin becomes.

Figure 4 shows the temperature adaptation performance of the hybrid e-skin in different environmental temperatures from 10 to 45°C. The e-skin was initially at 20°C, with a wind speed of 0.5 m s⁻¹. The auxiliary water was switched on after 5 min to change the air temperature, and the PID control system switch was turned on at the same time. The PID control system was turned off when the surface temperature of the e-skin exceeded the setpoint value. Figure 4A–C show the temperature adaptation process of the as-fabricated hybrid e-skin exposed to wind temperatures of 10, 25, 40°C, respectively. When the wind temperature was 10°C, the e-skin surface temperature quickly rose to 35°C, which is in the human body's comfort zone, and then sustained this temperature for a long time. However, the surface temperature of the prosthesis decreased with a change of the ambient temperature, ultimately reaching 12.5°C, which significantly deviated from a comfortable human body temperature. Similarly, under a wind temperature of 25°C, the e-skin maintained the target temperature, but the final surface temperature of the prosthesis was only 25°C. In a high temperature environment (40°C), the e-skin underwent both heating and cooling processes. The surface

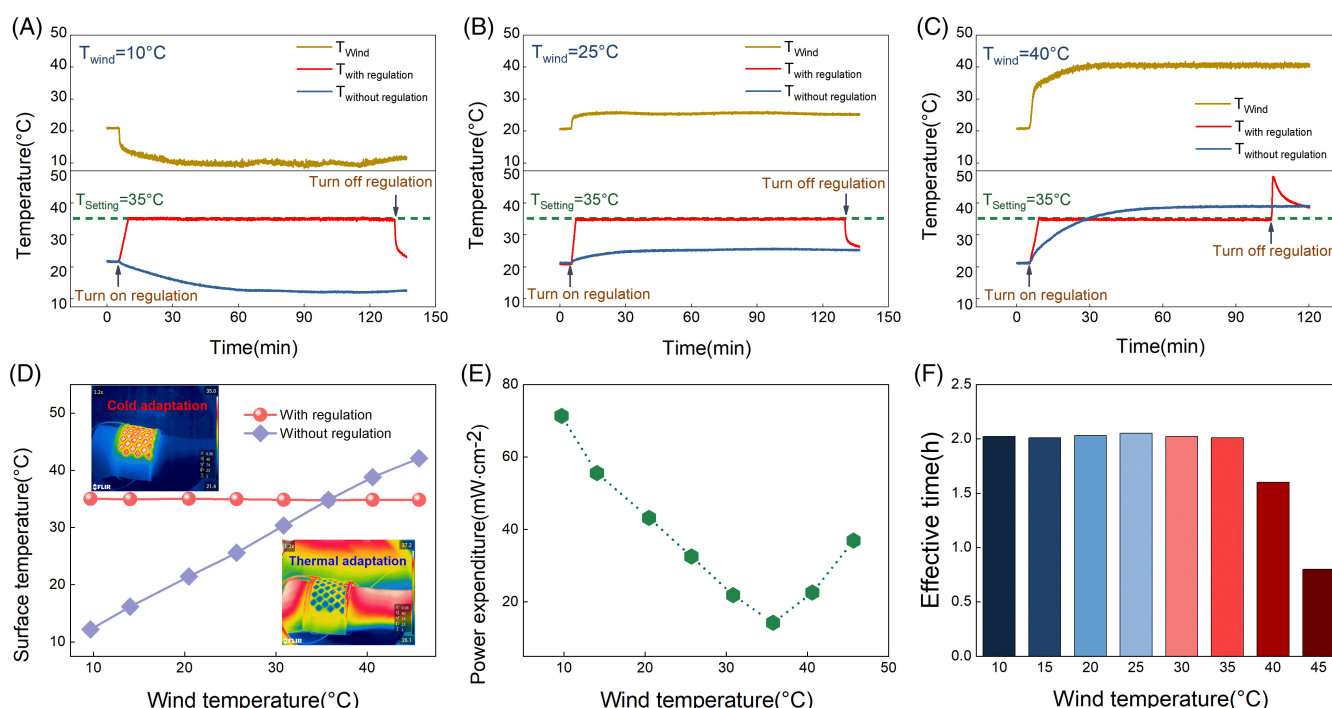


FIGURE 4 Temperature adaptation performance of the e-skin. (A) Temperature adaptation of the e-skin at low temperature; (B) temperature adaptation of the e-skin at room temperature; (C) temperature adaptation of the e-skin at high temperature; (D) effects of temperature adaptation on artificial limbs; (E) the power expenditure of the e-skin to maintain the surface temperature at 35°C at different ambient temperatures; (F) the effective time of temperature adaptation under different ambient temperatures

temperature of the e-skin rose rapidly, and once the e-skin overall temperature reached 35°C, it initiated surface cooling to maintain the target temperature. The temperature adaptation would ultimately be ineffective if the heat generated by the hot side exceeded the heat capacity of the phase change material. The surface temperature of the prosthesis, on the other hand, increased rapidly as the ambient temperature rose, exceeding 35°C at 28th min, and eventually reached 39°C. Figure 4D compares the temperature adaptation performance with and without regulation. With the power on, the as-fabricated e-skin displayed thermostatic functioning similar to humans, with an e-skin surface temperature of 35°C in the experimental temperature range of 10–45°C. In contrast, without power, the hybrid e-skin displayed weak temperature adaptation, showing a heterothermal-like surface temperature response proportional to the ambient temperature. The inset of Figure 4D also shows two infrared images of the e-skin in the power-on mode, at temperatures of 20 and 40°C.

Figure 4E shows the power expenditure of the e-skin required to maintain the surface temperature at 35°C at various wind temperatures. The power expenditure was calculated as the average power density of the e-skin for 10 min after the surface temperature stabilized at 35°C. At 10°C, the power expenditure of the e-skin was 71.32 mW cm⁻². The power expenditure gradually declined as the ambient temperature rose, reaching a minimum power expenditure (14.22 mW cm⁻²) at 35°C. Then, as the ambient temperature continued to rise, the e-skin began to cool, which caused power expenditure to gradually rise, reaching 36.91 mW cm⁻² at 45°C. This pattern is analogous to the energy expenditure of behavioral temperature regulation in humans at various ambient temperatures.³⁹ Homeotherms have a thermoneutral zone, which is the range of ambient temperatures in which oxygen consumption is the lowest and does not vary with ambient temperature. The further the ambient temperature deviates from the thermoneutral zone, the higher the expense of maintaining a constant temperature. The thermoneutral zone of the e-skin is approximately 35°C. By adjusting the target temperature, heat dissipation condition, or the heat exchange between the environment and the e-skin, the energy consumption and thermal neutral zone of the e-skin can be altered. Under diverse conditions, the effective time of temperature adaptation by the e-skin is shown in Figure 4G. The e-skin only performs heating when the ambient temperature is equal to or lower than the target temperature and the heat created can be released into the environment without impacting the e-skin's thermoregulating function. Here, the e-skin exhibited thermostatic control for the duration of the experiment (2 h) and can theoretically

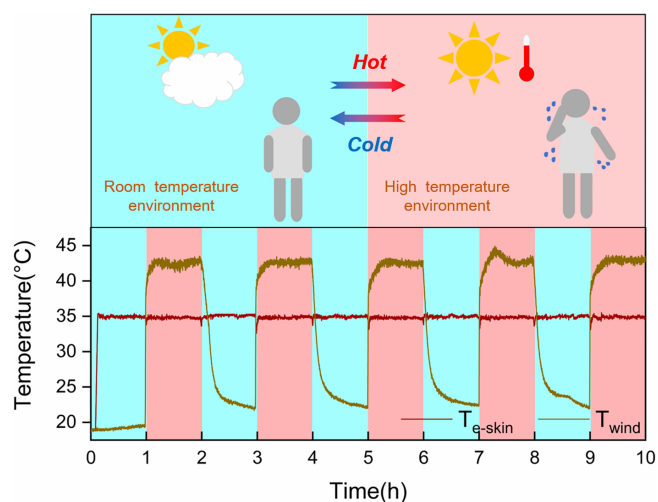


FIGURE 5 The hybrid e-skin maintained agile temperature regulation in a test of cycling low- and high-temperature environments.

maintain a surface temperature of 35°C indefinitely at low temperatures. When the ambient temperature is higher than the target temperature, the heat generated by the cooling process of the e-skin affects the temperature adaptation capacity of the e-skin. Nonetheless, under a wind temperature of 40°C, the hybrid e-skin was well regulated for 1.5 h, indicating good surface temperature adaptation.

Finally, we investigated the temperature adaptation performance of the as-fabricated hybrid e-skin in a scenario mimicking a person quickly moving between inside and outside temperatures (room-inside and room-outside) on a hot summer day. Here, we also used our wind channel to simulate the switching scenario, as shown in Figure 5. First, we kept the e-skin at the room-inside temperature (22°C) for 1 h. Next, hot air flow was used to heat the environment to the room-outside temperature (42°C). The skin quickly switched from cold-environment regulation to hot-environment regulation within 1 min under control of the PID feedback circuit. The temperature of the e-skin surface was then maintained consistently at 35°C. After 1 h in the room-outside temperature (42°C), cold air flow was used to return to the room-inside temperature (22°C). The as-fabricated hybrid e-skin also performed well in the reverse direction, showing rapid temperature adaptation within 1 min. This suggests that the as-fabricated e-skin with a hybrid flexible thermoelectric device and phase change material heat sink is a promising solution to mimic the temperature adaptation capability of human skin. Figure S2 depicts the temperature adaptation of e-skin in a windless environment. In a windless setting, the e-skin has a weaker heat exchange with the environment than in a windy environment,

hence temperature adaptability is improved. The power expenditure of maintaining 35°C in room temperature environment is lower (33.31 mW cm⁻²), and the effective time of maintaining 35°C in high temperature environment is longer (70 min).

3 | CONCLUSION

In this study, we developed a hybrid e-skin based on a thermoelectric device and phase change material heat sink, which provided controllable temperature adaptation in complex temperature environments and can be used to regulate the temperature of prosthetic limbs, thereby improving the experience of the wearer. The design of thermoelectric units and island-bridge circuits improved the flexibility of the e-skin, while the presence of paraffin wax provided a storage pool for the heat generated by the thermoelectric device. The specific power expenditure of the e-skin for heating and cooling under different environmental conditions was studied. In the case of wind speed of 0.5 m s⁻¹ and wind temperature of 10°C, the specific power expenditure of the e-skin is 8.53 mW cm⁻² °C⁻¹; in the case of wind speed of 0.5 m s⁻¹ and wind temperature of 45°C, the specific power expenditure of the e-skin is 7.3 mW cm⁻² °C⁻¹. The e-skin also imitated the thermostatic function of human skin, demonstrating the ability to maintain a comfortable surface temperature of 35°C over a wide ambient temperature range of 10–45°C. Its power expenditure was similar to that of the human body under different conditions. The power expenditure was larger when the environment deviated from the thermoneutral zone (71.32 mW cm⁻² at an ambient temperature of 10°C), and the power expenditure reached a minimum in the thermoneutral zone (14.22 mW cm⁻² at an ambient temperature of 35°C). The surface temperature of the e-skin was maintained at the target temperature for 2 h when the target was greater than the ambient temperature. While the ambient temperature was higher than the target temperature, the maintenance time was limited by the heat capacity of the phase change material, but the e-skin was still able to maintain the surface temperature at 35°C for nearly 1.5 h in a temperature of 40°C, 0.75 h even in 45°C, an extremely hot environment. Our hybrid e-skin also have a quick response in a scenario mimicking a person quickly moving between inside and outside temperatures (room-inside, 22°C and room-outside 42°C) on a hot summer. The e-skin had an effective temperature regulation capability and offered a novel option for the future generation of intelligent prosthetic temperature simulation, which was critical for improving the quality of life for amputees and for furthering bionic research of robots.

4 | EXPERIMENTAL SECTION

4.1 | Fabrication of the flexible thermoelectric device

The flexible thermoelectric device was used to manage the surface temperature of the e-skin in an active and bidirectional manner. The core of the flexible thermoelectric device is a flexible circuit. Flexible copper electrodes with a thickness of 100 µm were fabricated on a polyimide substrate by an electroplating process, and then the substrate, which did not cover the electrode, was removed by laser cutting. The devices were made using commercially sourced, 1.5 × 1.5 × 1.6 mm sized p-type Bi_{0.39}Sb_{1.61}Te_{3.03} legs and n-type Bi_{1.95}Te_{2.8}Se_{0.2} legs (Guangdong Fuxin Technology Co., Ltd. The related properties of thermoelectric materials are shown in Tables S1 and S2 of Supporting Information.). Two pairs of P and N thermoelectric legs were alternately welded on the copper electrode to create a thermoelectric unit, which was then connected with a flexible circuit (Figure S3A). The flexible circuit was placed on the same side of the thermoelectric device, allowing it to bend in both directions to satisfy its application requirements on prosthetic surfaces.

4.2 | Fabrication of the PCM heat sink

Paraffin is a suitable phase change material because it can absorb a large amount of heat while remaining stable around the phase change point. However, paraffin wax has a low thermal conductivity, which limits its heat absorption ability. Furthermore, due to irregular cooling speeds, paraffin wax will distort during the heating and cooling process. As a result, a frame with a high thermal conductivity was required to encapsulate the paraffin material. Porous foam is the appropriate construction material for a high thermal conductivity framework because of its flexibility and customizable porosity.^{40–43} Therefore, paraffin with a phase transition temperature of 37°C (Hangzhou RuhrTech Co., Ltd.) and commercial heat conductive potting adhesive with a thermal conductivity of 2 W mK⁻¹ were used to manufacture the PCM heat sink. Figure S3B depicts the flow diagram of the heat storage module fabrication process. An inverted mold of white sugar was used to create a foam structure from the potting sealant. This produced a foam structure with high thermal conductivity and porosity up to 65%. The PCM heat sink was completed when the paraffin melted into the thermal foam around body temperature at the phase transition point.

4.3 | Encapsulation of thermoregulating e-skin

The two modules were enclosed after being fabricated. To inhibit any undesired bypass heat transmission from the hot side to the cold side during the operation of the thermoelectric device, the flexible thermoelectric device was packed with low thermal conductivity aerogel/PDMS composites. For faster heat transfer, the flexible thermoelectric device and PCM heat sink were encapsulated with the heat conductive potting adhesive. The effective size of the temperature-controlled e-skin was approximately $67 \times 48 \times 4$ mm.

AUTHOR CONTRIBUTION

W.L. and P.Z. conceived the idea. P.Z. and B.D. designed the experiments, fabricated the devices, and performed the measurements. K.Z. analyzed the simulated mechanical performance. Q.Z., S.Z., and W.S. participated in the establishment of test equipment. P.Z., W.L. and Z.Z. wrote the manuscript, and all authors reviewed and commented on the manuscript.

ACKNOWLEDGMENTS

The authors acknowledge Guangdong Innovative and Entrepreneurial Research Team Program (No. 2016ZT06G587), Shenzhen Science and Technology Program (No. KYDPT20181011104007, GXWD20201230110313001), The Hong Kong Polytechnic University (Project ZVQM), and RGC Senior Research Fellow Scheme (SRFS21 22-5S04) for financial support of this work.

CONFLICT OF INTEREST

Zijian Zheng is Editor-in-Chief of *EcoMat* and co-author of this article. He was excluded from the peer-review process and all editorial decisions related to the acceptance and publication of this article. Peer-review was handled independently by another Associate Editor to minimize bias.

ORCID

Pengxiang Zhang  <https://orcid.org/0000-0001-8888-4856>

REFERENCES

- Lederman SJ, Klatzky RL. Haptic perception: A tutorial. *Atten Percept Psychophys*. 2009;71(7):1439-1459.
- Chortos A, Liu J, Bao ZA. Pursuing prosthetic electronic skin. *Nat Mater*. 2016;15(9):937-950.
- Abaira VE, Ginty DD. The sensory neurons of touch. *Neuron*. 2013;79(4):618-639.
- Kim JJ, Wang Y, Wang HY, Lee S, Yokota T, Someya T. Skin electronics: next-generation device platform for virtual and augmented reality. *Adv Funct Mater*. 2021;31(39):2009602.
- Hammock ML, Chortos A, Tee BCK, Tok JBH, Bao ZA. 25th anniversary article: the evolution of electronic skin (e-skin): a brief history, design considerations, and recent progress. *Adv Mater*. 2013;25(42):5997-6037.
- Yang JC, Mun J, Kwon SY, Park S, Bao ZN, Park S. Electronic skin: recent progress and future prospects for skin-attachable devices for health monitoring, robotics, and prosthetics. *Adv Mater*. 2019;31(48):1904765.
- Heikenfeld J, Jajack A, Rogers J, et al. Wearable sensors: modalities, challenges, and prospects. *Lab Chip*. 2018;18(2):217-248.
- Sun C, Wang X, Auwalu MA, Cheng S, Hu W. Organic thin film transistors-based biosensors. *EcoMat*. 2021;3(2):e12094.
- Tao X, Liao S, Wang Y. Polymer-assisted fully recyclable flexible sensors. *EcoMat*. 2021;3(2):e12083.
- Li Q, Zhang LN, Tao XM, Ding X. Review of flexible temperature sensing networks for wearable physiological monitoring. *Adv Healthc Mater*. 2017;6(12):1601371.
- Hong SY, Lee YH, Park H, et al. Stretchable active matrix temperature sensor array of polyaniline nanofibers for electronic skin. *Adv Mater*. 2016;28(5):930-935.
- Su Y, Ma CS, Chen J, et al. Printable, highly sensitive flexible temperature sensors for human body temperature monitoring: a review. *Nanoscale Res Lett*. 2020;15(1):1-34.
- Craig A. Pain mechanisms: labeled lines versus convergence in central processing. *Annu Rev Neurosci*. 2003;26(1):1-30.
- Guyton AC, Hall JE. Metabolism and temperature regulation. In: Guyton AC, Hall JE, eds. *Textbook of medical physiology*. Philadelphia: Saunders, 1986:829-901.
- Lillywhite HB. Behavioral temperature regulation in bullfrog, *rana-catesbeiana*. *Copeia*. 1970;1970(1):158-168.
- Tabor J, Chatterjee K, Ghosh TK. Smart textile-based personal thermal comfort systems: current status and potential solutions. *Adv Mater Technol*. 2020;5(5):1901155.
- Gibbons MJ, Marengo M, Persoons T. A review of heat pipe technology for foldable electronic devices. *Appl Therm Eng*. 2021;194(July):117087.
- Moore AL, Shi L. Emerging challenges and materials for thermal management of electronics. *Mater Today*. 2014;17(4):163-174.
- Fu YF, Hansson J, Liu Y, et al. Graphene related materials for thermal management. *2D Mater*. 2020;7(1):012001.
- Balandin AA. Thermal properties of graphene and nanostructured carbon materials. *Nat Mater*. 2011;10(8):569-581.
- Ali Z, Gao Y, Tang B, et al. Preparation, properties and mechanisms of carbon fiber/polymer composites for thermal management applications. *Polymers*. 2021;13(1):169.
- Shi YL, Wang CJ, Yin YF, Li YH, Xing YF, Song JZ. Functional soft composites as thermal protecting substrates for wearable electronics. *Adv Funct Mater*. 2019;29(45):1905470.
- Umair MM, Zhang Y, Iqbal K, Zhang SF, Tang BT. Novel strategies and supporting materials applied to shape-stabilize organic phase change materials for thermal energy storage—a review. *Appl Energy*. 2019;235(February):846-873.
- Kou Y, Sun KY, Luo JP, et al. An intrinsically flexible phase change film for wearable thermal managements. *Energy Storage Mater*. 2021;34(January):508-514.
- Tong JK, Huang XP, Boriskina SV, Loomis J, Xu YF, Chen G. Infrared-transparent visible-opaque fabrics for wearable personal thermal management. *ACS Photonics*. 2015;2(6):769-778.
- Hsu PC, Song AY, Catrysse PB, et al. Radiative human body cooling by nanoporous polyethylene textile. *Science*. 2016;353(6303):1019-1023.

27. Zeng SN, Pian SJ, Su MY, et al. Hierarchical-morphology meta-fabric for scalable passive daytime radiative cooling. *Science*. 2021;373(6555):692-696.
28. Hsu PC, Liu C, Song AY, et al. A dual-mode textile for human body radiative heating and cooling. *Sci Adv*. 2017;3(11):e1700895.
29. Choi S, Park J, Hyun W, et al. Stretchable heater using ligand-exchanged silver nanowire nanocomposite for wearable articular thermotherapy. *ACS Nano*. 2015;9(6):6626-6633.
30. Hong S, Lee H, Lee J, et al. Highly stretchable and transparent metal nanowire heater for wearable electronics applications. *Adv Mater*. 2015;27(32):4744-4751.
31. Im K, Cho K, Kwak K, Kim J, Kim S. Flexible transparent heaters with heating films made of indium tin oxide nanoparticles. *J Nanosci Nanotechnol*. 2013;13(5):3519-3521.
32. Hsu PC, Liu X, Liu C, et al. Personal thermal management by metallic nanowire-coated textile. *Nano Lett*. 2015;15(1):365-371.
33. Zhao DL, Lu X, Fan TZ, et al. Personal thermal management using portable thermoelectrics for potential building energy saving. *Appl Energy*. 2018;218(May):282-291.
34. Kishore RA, Nozariasbmarz A, Poudel B, Sanghadasa M, Priya S. Ultra-high performance wearable thermoelectric coolers with less materials. *Nat Commun*. 2019;10(1):1-13.
35. Russ B, Glaudell A, Urban JJ, Chabiny ML, Segalman RA. Organic thermoelectric materials for energy harvesting and temperature control. *Nat Rev Mater*. 2016;1(10):1-14.
36. Hong S, Gu Y, Seo JK, et al. Wearable thermoelectrics for personalized thermoregulation. *Sci Adv*. 2019;5(5):eaaw0536.
37. Gagge AP, Stolwijk J, Hardy J. Comfort and thermal sensations and associated physiological responses at various ambient temperatures. *Environ Res*. 1967;1(1):1-20.
38. Kingma BR, Frijns AJ, Schellen L, van Marken Lichtenbelt WD. Beyond the classic thermoneutral zone: including thermal comfort. *Temperature*. 2014;1(2):142-149.
39. Terrien J, Perret M, Aujard F. Behavioral thermoregulation in mammals: a review. *Front Biosci*. 2011;16(1):1428-1444.
40. Choi SJ, Kwon TH, Im H, et al. A polydimethylsiloxane (pdms) sponge for the selective absorption of oil from water. *ACS Appl Mater Interfaces*. 2011;3(12):4552-4556.
41. Li HS, Ding Y, Ha H, et al. An all-stretchable-component sodium-ion full battery. *Adv Mater*. 2017;29(23):1700898.
42. Liu W, Chen Z, Zhou GM, et al. 3D porous sponge-inspired electrode for stretchable lithium-ion batteries. *Adv Mater*. 2016;28(18):3578-3583.
43. Song Y, Chen HT, Su ZM, et al. Highly compressible integrated supercapacitor-piezoresistance-sensor system with CNT-PDMS sponge for health monitoring. *Small*. 2017;13(39):1702091.

SUPPORTING INFORMATION

Additional supporting information can be found online in the Supporting Information section at the end of this article.

How to cite this article: Zhang P, Deng B, Zhu K, et al. Wide-temperature range thermoregulating e-skin design through a hybrid structure of flexible thermoelectric devices and phase change materials heat sink. *EcoMat*. 2022; 4(6):e12253. doi:[10.1002/eom2.12253](https://doi.org/10.1002/eom2.12253)